


Imaging Reconfigurable Molecular Concentration on a Graphene Field-Effect Transistor

Franklin Liou,[◆] Hsin-Zon Tsai,[◆] Andrew S. Aikawa, Kyler C. Natividad, Eric Tang, Ethan Ha, Alexander Riss, Kenji Watanabe, Takashi Taniguchi, Johannes Lischner, Alex Zettl, and Michael F. Crommie*

 Cite This: *Nano Lett.* 2021, 21, 8770–8776

 Read Online

ACCESS |

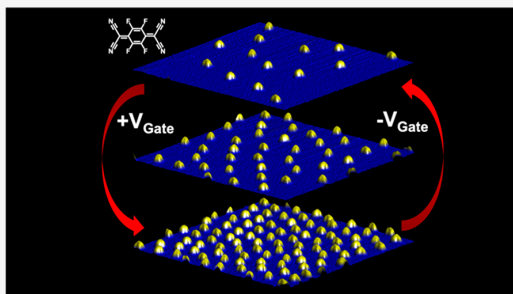
 Metrics & More

 Article Recommendations

 Supporting Information

ABSTRACT: The spatial arrangement of adsorbates deposited onto a clean surface under vacuum typically cannot be reversibly tuned. Here we use scanning tunneling microscopy to demonstrate that molecules deposited onto graphene field-effect transistors (FETs) exhibit reversible, electrically tunable surface concentration. Continuous gate-tunable control over the surface concentration of charged F_4TCNQ molecules was achieved on a graphene FET at $T = 4.5\text{ K}$. This capability enables the precisely controlled impurity doping of graphene devices and also provides a new method for determining molecular energy level alignment based on the gate-dependence of molecular concentration. Gate-tunable molecular concentration is explained by a dynamical molecular rearrangement process that reduces total electronic energy by maintaining Fermi level pinning in the device substrate. The molecular surface concentration is fully determined by the device back-gate voltage, its geometric capacitance, and the energy difference between the graphene Dirac point and the molecular LUMO level.

KEYWORDS: Fermi level pinning, graphene field-effect device, molecular electronics, gate-tunable adsorbates



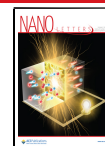
INTRODUCTION

One important way in which adsorbates modify surfaces is by inducing localized electronic defect states that trap electrons and cause Fermi level pinning.^{1–4} Typically, Fermi level pinning is considered a “one-way” process where defects may change the location of electrons (i.e., by trapping them) but electrons do not change the location of defects. Here we reverse this idea by implementing a condensed matter system where the defect concentration can be continuously and reversibly tuned by adding or removing electrons from the system. We observe this unique behavior for Tetrafluoro-tetracyanoquinodimethane (F_4TCNQ) molecules adsorbed onto the surface of a graphene field-effect transistor (FET). When voltage is applied to the back-gate of such a device under proper conditions, then the resulting electric field is not screened by the graphene Dirac band electrons but rather is unexpectedly screened by ionized molecules that mechanically rearrange themselves on the device surface. The devices in which this occurs are not electrochemical cells^{5–7} attached to some external reservoir of material. Instead they are composed of ultraclean monolayers of graphene on hBN that are dosed with a submonolayer molecular coverage and then held at cryogenic temperature under ultrahigh vacuum (UHV). The adsorbate rearrangement process observed on our devices arises from a physical mechanism whereby adsorbate-induced

Fermi level pinning helps to minimize graphene Dirac band electronic energy. The energetics of Fermi level pinning in this 2D system is so strongly tied to the adsorbate arrangement that it allows reversible, mechanical alteration of the surface defect concentration by adding or removing electrons using the FET back-gate.

This behavior arises due to the proximity in energy of the F_4TCNQ lowest unoccupied molecular orbital (LUMO) to the graphene Dirac point.^{8–12} The resulting high electron affinity of F_4TCNQ on graphene has been exploited previously to p-dope graphene.^{13,14} Scanning tunneling microscopy (STM) measurements have also shown that charge flows easily into and out of F_4TCNQ molecules on graphene.^{8,10,15,16} No previous studies, however, have demonstrated reversible control over the geometric arrangement of F_4TCNQ adsorbates on graphene.

Received: August 6, 2021
Revised: October 12, 2021
Published: October 15, 2021



The strategy of this paper is to first explain the experimental procedure by which we control the surface concentration of F_4TCNQ molecules on a graphene FET via electrical signals sent to the device. This technique has enabled us to discover that the F_4TCNQ surface concentration on graphene FETs varies linearly with applied gate voltage. We have characterized this unexpected behavior by performing STM and scanning tunneling spectroscopy (STS) on molecule-decorated graphene devices for different molecular coverages. These measurements allow us to establish a connection between a gate-dependent molecular surface concentration and Fermi level pinning in graphene FETs. We have distilled these observations into a simple theoretical model that connects the energetics of graphene electrons to the geometric arrangement of surface adsorbates, which allows us to predict molecular surface concentration for any given back-gate voltage. The connection established here between molecular electronic structure and molecular surface concentration provides a new technique for quantitatively determining molecular energy levels by simply counting the number of molecules on a clean graphene surface.

RESULTS

Our technique for reversibly changing molecular concentration on graphene devices starts with the deposition of a submonolayer coverage of F_4TCNQ molecules onto a clean graphene/hBN FET held at room temperature under UHV (the transconductance of the pristine device and an SEM image are shown in Figure S1). We then cool the molecule-decorated device down to 4.5 K without breaking vacuum, at which point the molecules can be stably imaged by our STM. In order to set the molecular surface concentration to a desired value, a set-voltage (V_{G-set}) is applied to the device back-gate while a source-drain current (I_{SD}) is simultaneously passed through the graphene as sketched in Figure 1 (I_{SD} provides thermal energy to facilitate molecular diffusion). The molecules freeze in place as soon as I_{SD} is set to zero, resulting in a well-defined and reversible surface concentration that is determined by V_{G-set} . After the molecules are frozen in place, the gate voltage is set to zero for STM imaging (see Supporting Information Note 2). The resulting control over the molecular surface concentration can be seen in the differently prepared molecular concentrations shown in Figures 2a–f (all measured at the same spot on the surface). At a high set-voltage of $V_{G-set} = 60$ V, the resulting molecular surface concentration is correspondingly high ($n_M = 6 \times 10^{12} \text{ cm}^{-2}$), and the roughly evenly spaced molecular distribution suggests that the molecules are charged during the surface-concentration-setting process and repel each other (Figure 2a). As V_{G-set} is reduced, the resulting molecular concentration correspondingly reduces (Figure 2b–f). A plot of molecule surface concentration versus V_{G-set} (Figure 2g) shows that the molecular concentration is almost perfectly linear over the gate-voltage range $-10 \text{ V} < V_{G-set} < 60 \text{ V}$ and remains nearly zero for $V_{G-set} < -10 \text{ V}$. The gate-tunable molecular concentration is observed to be nonhysteretic since the forward sweep and backward sweep data lie almost perfectly on top of each other. The molecular concentration within our STM field of view is thus precisely and reversibly controlled by tuning the graphene FET electrical device parameters.

The molecular concentration across the entire device surface, however, cannot be completely uniform since the molecules have to go *somewhere* when their concentration is

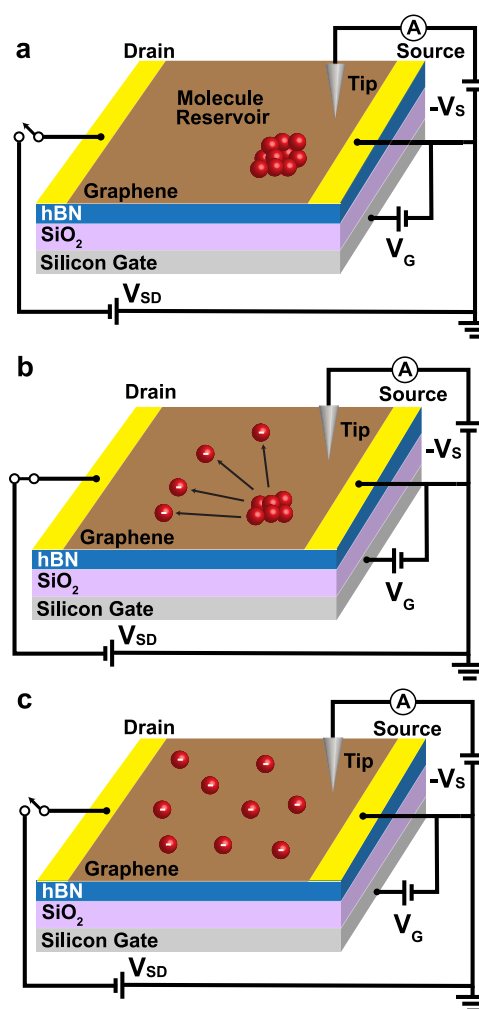


Figure 1. Controlling molecular concentration on a graphene field-effect transistor (FET). (a) Sketch representing the F_4TCNQ molecular configuration (red balls) in the “as-grown” state after thermal evaporation onto a graphene FET. A representative circuit shows the biases applied to the device. (b) Application of a back-gate voltage of $V_G = V_{G-set}$ to the FET, while simultaneously flowing a source–drain current I_{SD} through the graphene causes the molecules to diffuse out onto the graphene surface. Typical values of V_{G-set} range from -60 to 60 V. Typical values of V_{SD} used for changing the molecular concentration range from 2 to 6 V, and typical I_{SD} values range from 0.5 to 2 mA. (c) When the source-drain current is turned off the device cools and the molecules freeze in place. The gate voltage V_G is then returned to 0 V, and a sample bias (relative to the tip) of $V_s = 2$ V with current set point of 2 pA can then be used for stably scanning the molecules.

reduced and come back from somewhere when their concentration is increased, and this “somewhere” cannot have the same concentration as the STM field of view seen in Figure 2. However, the process described above for setting the molecular surface concentration is surprisingly robust and can be observed over a majority of the surface area that we have scanned ($\sim 80\%$) on multiple devices. A fraction of the device surface is defective/contaminated ($\sim 20\%$) (and therefore unsuitable for these measurements) since the devices are

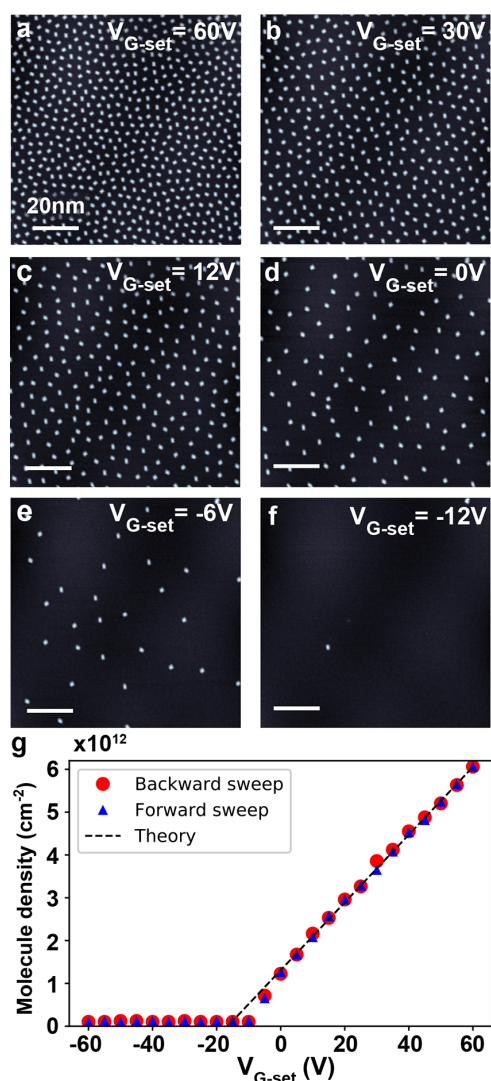


Figure 2. Tuning molecular concentration by using FET gate voltage: (a–f) STM topographs of the same area on the surface of a graphene field-effect transistor after tuning the molecular surface concentration with different values of gate set-voltage over the range $-12\text{ V} < V_{\text{G-set}} < 60\text{ V}$. (g) Measured molecular concentration as a function of $V_{\text{G-set}}$. No hysteresis is observed for forward and backward sweeps. The dashed line shows a theoretical fit to the data using eq 5.

fabricated under ambient conditions before being placed in our UHV chamber for measurement. We hypothesize that defective regions of the surface act as *local reservoirs* that store F_4TCNQ molecules in a compact, condensed phase. F_4TCNQ molecules must flow in and out of these condensation regions (due to electrostatic potential inhomogeneities) to enable the precise concentration control that we observe over a large majority of the surface.

The fact that we observe no significant decrease in molecule concentration over multiple cycles of density changing operations (Figure S2) suggests that the molecular storage and release process is fully reversible. To explain why molecules aggregate in a condensed phase we hypothesize that a highly negative gate voltage draws electrons out of the

device and thus removes charge from the molecules. This reduces the repulsive Coulomb interactions between them, thereby causing attractive intermolecular forces (such as van der Waals) to become more dominant. Weak molecule–substrate interactions allow the molecules to diffuse easily to defective regions where they can be captured. A definitive test of this “local reservoir hypothesis” is difficult since mapping the entire surface of a graphene FET at the atomic scale is currently not possible (highly defective regions cannot be imaged), but we note that a condensed phase of F_4TCNQ molecules has been observed on F_4TCNQ -decorated graphene FETs in the past.¹⁷

In order to understand the microscopic mechanism that underlies the process of tuning molecular surface concentration we must understand how charge readjusts itself in a graphene device decorated by mobile, charge-tunable molecules as the gate voltage is changed. Here the molecule-decorated graphene forms one side of a capacitor while the back-gate electrode forms the other, so the total charge that flows to the molecule/graphene system can be determined straightforwardly from the device capacitance and applied gate-voltage ($Q_{\text{T}} = -V_{\text{G-set}}C_{\text{T}}$). Electrons transferred to the graphene side of the capacitor can either occupy graphene Dirac Fermion band states or, alternatively, the LUMO states of the adsorbed molecules. To clarify how charge is distributed between these two choices, we carried out STM spectroscopy directly on adsorbed F_4TCNQ molecules as well as on bare graphene patches between the molecules for different applied gate voltages and different molecular concentrations. This enabled us to track the energetic alignment of the F_4TCNQ LUMO energy (E_{L}) and the graphene Dirac point energy (E_{D}) with respect to the graphene Fermi level (E_{F}), thus providing snapshots of how charge in the device is distributed under different conditions. Our observations in this regard provide the basis for a simple model that quantitatively predicts the gate-tunable molecular surface concentration.

We first describe the negative gate voltage regime, $V_{\text{G}} < -10\text{ V}$, where the electronic configuration of the molecule/graphene system is qualitatively represented by the sketch in the inset to Figure 3c. Here the graphene is p-doped since E_{F} lies below E_{D} . The molecular LUMO level, E_{L} , lies below E_{D} but remains unfilled by electrons since it is still higher than E_{F} . Experimental evidence for this type of electronic behavior is seen in the “on-molecule” and “off-molecule” dI/dV_{S} spectra of Figure 3a,b, where V_{S} is the sample bias of the tunnel junction (all dI/dV_{S} spectra shown in Figure 3 were acquired after “freezing” the molecules by setting I_{SD} to zero; spectroscopy was never acquired under “diffusive” conditions where $I_{\text{SD}} \neq 0$). Molecular spectra are only shown for $V_{\text{S}} > 0$ since negative V_{S} induced tip electric fields that caused the molecules to charge and adsorb onto the tip. The top curve in Figure 3a shows an on-molecule dI/dV_{S} spectrum measured with the STM tip held above the center of an F_4TCNQ molecule for a gate voltage of $V_{\text{G}} = -60\text{ V}$ and a fixed molecular surface concentration of $n_{\text{M}} = 0.8 \times 10^{12}\text{ cm}^{-2}$ (see inset). The F_4TCNQ LUMO level (arrow) sits at a sample bias of $V_{\text{S}} \approx 0.2\text{ V}$ above the Fermi energy (which is at $V_{\text{S}} = 0$). The precise energy position of the LUMO is determined following the protocol of ref 8 after accounting for known inelastic tunneling effects (see Figure S3).^{8,18,19} We note that the each LUMO arrow is shifted slightly to the left of the spectrum maximum due to a 35 meV phonon mode (found by fitting high-resolution STS measurements as described in ref 8, see

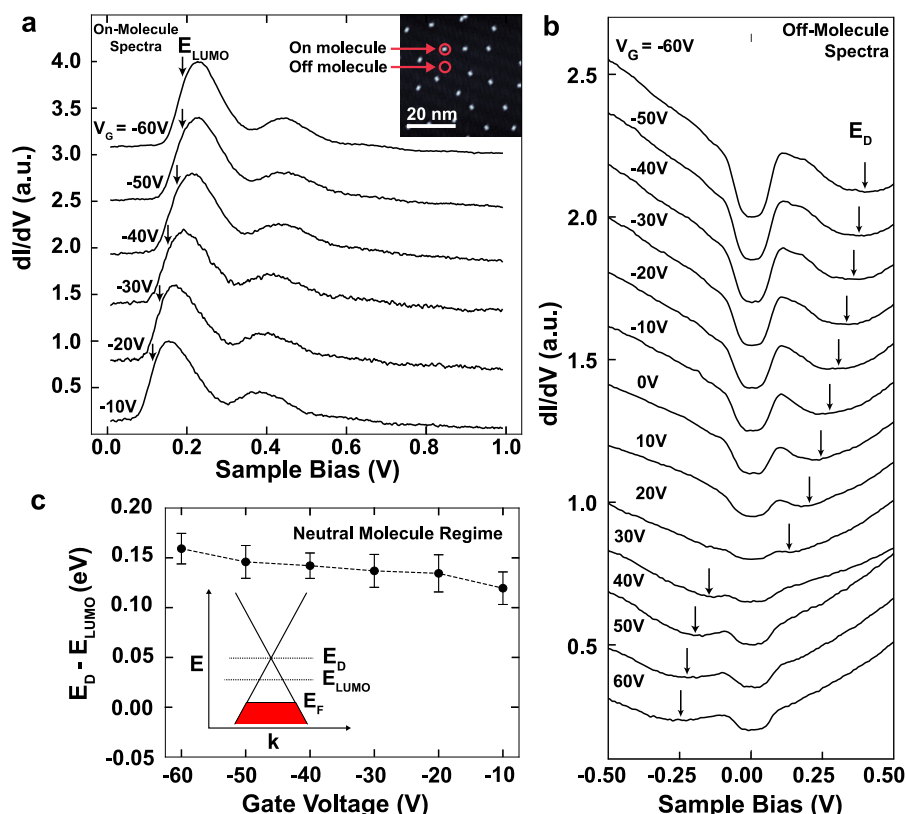


Figure 3. STM spectroscopy of F_4TCNQ -decorated graphene field-effect transistor (FET): (a) dI/dV_S spectra measured while holding the STM tip directly above an F_4TCNQ molecule for a molecular concentration of $0.8 \times 10^{12} \text{ cm}^{-2}$ at the surface of a graphene FET ($-60 \text{ V} < V_G < -10 \text{ V}$). Energy location of the lowest unoccupied molecular orbital (E_L) is marked. Inset shows a representative image of the surface at this molecular concentration. (b) dI/dV_S spectra measured while holding the STM tip over bare patches of graphene $\sim 100 \text{ \AA}$ away from nearby F_4TCNQ molecules for the same surface conditions measured in (a) ($-60 \text{ V} < V_G < 60 \text{ V}$, $n_M = 0.8 \times 10^{12} \text{ cm}^{-2}$). Graphene Dirac point energy (E_D) is marked. Spectroscopy parameters: $I_{\text{set-point}} = 50 \text{ pA}$, $V_{\text{set-point}} = 1 \text{ V}$ on graphene, $I_{\text{set-point}} = 10 \text{ pA}$, and $V_{\text{set-point}} = 1 \text{ V}$ on molecule. (c) Gate-voltage dependence of the Dirac point energy relative to the molecular LUMO energy ($E_D - E_L$) for molecular concentration $n_M = 0.8 \times 10^{12} \text{ cm}^{-2}$. Inset shows a simplified representation of the electronic structure of F_4TCNQ molecules on graphene for large negative gate voltages (E_F = Fermi energy).

Supporting Information Note 4) that broadens the LUMO peak⁸ and results in the LUMO energy being lower than the apparent maximum by $\sim 35 \text{ meV}$. A previously reported satellite peak due to a 183 meV phonon mode is also visible at $V_S \approx 0.4 \text{ V}$.⁸

The top curve in Figure 3b shows an off-molecule dI/dV_S spectrum taken with the STM tip held over a bare patch of graphene $\sim 100 \text{ \AA}$ away from any F_4TCNQ molecules for the same gate-voltage and molecular concentration used for the top curve of Figure 3a. A depression in dI/dV_S over the range $-60 \text{ mV} < V_S < 60 \text{ mV}$ can be seen that is known to occur due to phonon inelastic tunneling effects,²⁰ while another depression is seen at $V_S \approx 0.35 \text{ V}$ that marks the location of the graphene Dirac point (E_D).^{20,21} The precise value of E_D is found by fitting the dI/dV_S spectra using the protocol outlined in the Supporting Information. The Dirac point is seen to fall in energy as the gate voltage is increased, causing the graphene to transition from being hole-doped ($E_D > E_F$) to being electron-doped ($E_D < E_F$) at $V_G \approx 20 \text{ V}$ for this molecular surface concentration ($n_M = 0.8 \times 10^{12} \text{ cm}^{-2}$). E_D (from Figure 3b) is observed to lie above E_L (from Figure 3a) by $\sim 150 \text{ mV}$ for negative gate voltages, and both quantities shift downward

in energy together as the gate voltage is increased from $V_G = -60 \text{ V}$ to -10 V (Figure 3c). Such behavior is expected as E_F “rises” with increased gate voltage in the band structure shown in the inset to Figure 3c.

When V_G is raised above -10 V , the molecules become charged, causing them to enter a new physical regime. The transition toward this regime can be seen in the gate-dependence of E_L , which falls toward E_F with increasing V_G in Figure 3a. Another sign that the molecules have become charged (i.e., that the LUMO becomes filled) is that they become mechanically unstable during STS measurement when V_G is raised above -10 V . Negatively charged molecules are observed to escape from under the STM tip during spectroscopy measurements, making it impossible to obtain reproducible “on-molecule” spectroscopy for $V_G > -10 \text{ V}$. Interestingly, this critical gate-voltage value coincides with the $V_{G\text{-set}}$ value at which the molecular concentration begins to rise from near zero (for increasing $V_{G\text{-set}}$), showing that the appearance of molecules on the device surface is correlated with their charge state. Another indication of charged molecular behavior is the spatially uniform intermolecular separation, a signature of intermolecular repulsion.

In order to better understand the charged molecular regime, we investigated how changing the molecular surface concentration affects the way electrons fill up graphene states during electrostatic gating. This was accomplished by inspecting the gate-dependence of E_D for different fixed molecular concentrations. Such measurements reveal charge transfer to F₄TCNQ LUMO levels and how this leads to Fermi-level pinning. To see this, we first set the molecular concentration to a desired value (as shown in Figure 4a) and then measured the

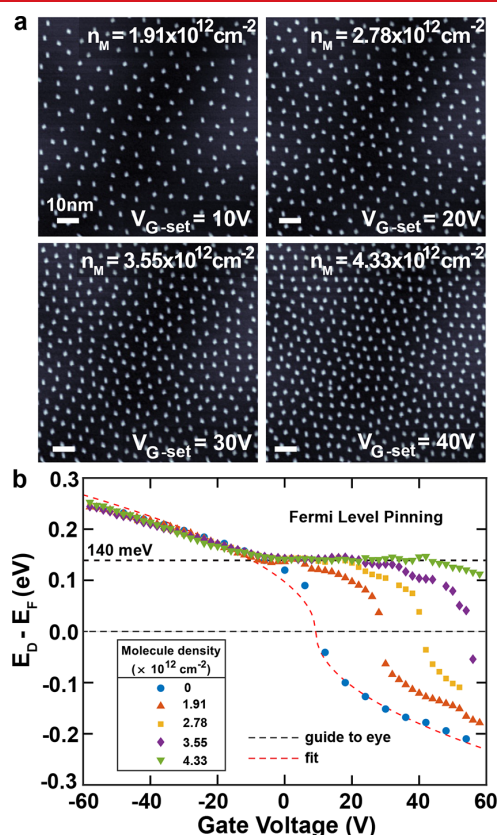


Figure 4. Fermi level pinning of F₄TCNQ-doped graphene field-effect transistor (FET): (a) STM images of graphene FET surface decorated with different molecular densities for measurement of molecule-induced Fermi-level pinning shown in (b). (b) Gate voltage dependence of Dirac point energy (E_D) measured via STS on graphene FET surface for the different molecular densities shown in (a). Concentration-dependent plateau in E_D indicates Fermi level pinning. Red dashed line shows the fit of eq 1 to data for zero molecular concentration ($n_M = 0$).

gate-voltage dependence of E_D (Figure 4b) using off-molecule dI/dV_S spectra via the procedure described above for Figure 3b. For a pristine graphene capacitor, E_D is expected to move smoothly down in energy with increasing V_G according to the well-known expression:²⁰

$$E_D(V_G) = -\text{sgn}(V_G) \hbar v_F \sqrt{\pi C |V_G - V_0|} \quad (1)$$

where $v_F = 1.1 \times 10^6 \text{ m/s}$ is the electron Fermi velocity in graphene, C is the unit area capacitance of the device, and V_0 reflects background doping. By fitting eq 1 to the gate-dependent Dirac point energy of our device before depositing

molecules, we are able to extract the capacitance between the graphene and the back-gate electrode: $C = (7.8 \pm 0.2) \times 10^{10} \text{ cm}^{-2} \text{ V}^{-1}$ (Figure S5).

For nonzero molecular concentrations, however, the E_D versus V_G curve deviates from eq 1 and forms a “pinning” plateau at $\sim 140 \text{ meV}$ above E_F , with the width of the plateau increasing with increased molecular surface concentration (Figure 4b). The start of the plateau (for increasing V_G) coincides with the gate voltage value where the molecular LUMO begins to fall under E_F , thus allowing us to associate the plateau with the charging of F₄TCNQ molecules. The value of E_D at the plateau ($\sim 140 \text{ meV}$ above E_F) is very close to the energy difference observed between E_D and E_L in Figure 3c, providing evidence that the Fermi level is pinned to the molecular LUMO level 140 meV below E_D . This interpretation is quantitatively supported by the increased width of the pinned region (in V_G) as molecular concentration is increased (i.e., since higher molecular concentrations can store more charge). For example, the E_D plateau at a fixed molecular concentration of $4.3 \times 10^{12} \text{ cm}^{-2}$ has a width of $\Delta V_G = 50 \pm 5 \text{ V}$, which corresponds to a surface charge density of $\Delta\sigma = (3.9 \pm 0.4) \times 10^{12} \text{ e}^-/\text{cm}^2$ that reasonably matches the molecular concentration (charge is calculated using the capacitance value acquired via eq 1).

The Fermi level pinning described above for the static molecular configurations of Figure 4a is intimately related to the dynamic molecular reconfigurations that enable molecular concentration to be continuously tuned by gate voltage, the central focus of this paper. When the graphene Fermi level is securely pinned by molecular LUMO states, new electrons added to the device (e.g., by an increase in V_G) do not cause the Fermi level to rise in energy since LUMO levels absorb any new charge added to the graphene at E_F . However, if there are not enough molecules on the surface to pin the Fermi level, then increasing the gate voltage causes electrons to occupy graphene band states at energies higher than E_L . This is the origin (from an energetic perspective) of the force that drives the molecules to move on the surface in order to dynamically change the molecular concentration when $V_{G\text{-set}}$ is modified under “diffusive conditions” (i.e., when $I_{SD} \neq 0$). When $V_{G\text{-set}}$ is increased under diffusive conditions, then the molecular concentration must also increase to maintain Fermi level pinning (the overall lowest energy state) so as to enable charge to flow into lower-energy LUMO levels rather than higher-energy Dirac band states.

These concepts allow us to formulate a simple model for predicting the expected concentration of molecules on the graphene surface for a given gate voltage. We start with the assumption that the lowest-energy electronic configuration under diffusive conditions (and when $-10 \text{ V} < V_G$) occurs when the Fermi energy is pinned at E_L . For a given value of $V_{G\text{-set}}$ the total charge density on the molecule-decorated FET surface ($\sigma_T = -CV_{G\text{-set}}$) will have contributions both from charge carried by the molecules (σ_M) and charge carried by the graphene Dirac band (σ_G):

$$-CV_{G\text{-set}} = \sigma_M + \sigma_G \quad (2)$$

If each charged molecule contains one electron in its LUMO state (assuming that double occupancy is forbidden due to the large Hubbard energy of the LUMO state),⁸ then the total molecular charge is $\sigma_M = -n_M$, where n_M is the surface concentration of molecules and σ_M has units of lel. Equation 2 then leads to the following expression for n_M :

$$n_M = CV_{G\text{-set}} + \sigma_G \quad (3)$$

Because E_F is pinned at E_L by the molecular coverage and $E_D - E_D < 0$, σ_G can be found by integrating the density of states in the graphene band from the Dirac point to E_L , resulting in the following well-known expression:²²

$$\sigma_G = \frac{|E_D - E_L|^2}{\pi \hbar^2 v_F^2} \quad (4)$$

Combining eqs 4 and 3 leads to the final expression for molecular concentration as a function of $V_{G\text{-set}}$:

$$n_M = CV_{G\text{-set}} + \frac{|E_D - E_L|^2}{\pi \hbar^2 v_F^2} \quad (5)$$

Using $v_F = 1.1 \times 10^6$ m/s, we are able to fit eq 5 to the n_M versus $V_{G\text{-set}}$ data of Figure 2g by using $|E_D - E_L|$ and C as fitting parameters. Equation 5 fits the data well for a value of $|E_D - E_L| = 142 \pm 23$ meV and a value of $C = (7.9 \pm 0.6) \times 10^{10}$ cm⁻² V⁻¹. This value of capacitance agrees well with our independently determined device capacitance of $C = (7.8 \pm 0.2) \times 10^{10}$ cm⁻² V⁻¹ (Figure S5). A consequence of the good agreement between these capacitance values is confirmation that each F₄TCNQ molecule carries a single electron of charge, since every additional electron accumulated by increasing the gate voltage corresponds to an additional molecule.

We can further check the validity of this conceptual framework by comparing the value of $E_D - E_L$ obtained from our molecular concentration measurements with the value obtained independently from the STS measurements shown in Figures 3 and 4. STS enables us to obtain $E_D - E_L$ in two ways: first, by extracting E_L and E_D directly from the dI/dV_S spectra in Figure 3a,b and subtracting them, and second, from the E_D energy plateau caused by Fermi level pinning in Figure 4. Using the first method we see from Figure 3 that for $V_G = -30$ V our on-molecule dI/dV_S spectrum yields $E_L = 165$ meV, while our off-molecule spectrum yields $E_D = 305$ meV. This results in a value of $E_D - E_L = 140 \pm 20$ meV (the average value over the gate-voltage range $-60 \text{ V} < V_G < -10 \text{ V}$ is $E_D - E_L = 143 \pm 9$ meV which remains quite close to this value). Using the second method, the Fermi-level pinning data of Figure 4 reveals a Dirac point plateau at $E_D - E_F = 140 \text{ meV} \pm 5$ meV. Since E_F is pinned at E_L under these conditions, this reflects a value of $E_D - E_L = 140 \text{ meV} \pm 5$ meV. Both methods are in agreement with the value $|E_D - E_L| = 142 \pm 23$ meV obtained from the concentration-based analysis of eq 5 and thus support the overall physical picture that we have presented.

One consequence of this analysis is that measurement of molecular concentration on a graphene FET is shown to provide a new method for quantitatively determining the energy of molecular frontier orbitals with respect to the graphene Dirac point (i.e., $E_D - E_L$). This new method is potentially valuable for determining the energy alignment of highly mobile adsorbates since it can be extremely difficult to prevent them from moving when they are under an STM tip during the bias sweeps required for STS (characterizing small devices can also be quite challenging for X-ray-based probes). In our previous work, for example, we found it necessary to anchor F₄TCNQ molecules to a secondary immobile molecular template in order to probe their LUMO levels in the charged state via STS.⁸ Such molecular templating, however, can alter local dielectric environments and influence

molecular orbital energies.^{23,24} Our new technique of measuring gate-dependent molecular concentrations allows one to bypass templating and to access molecular-energy-level information via a completely different method.

In conclusion, we have demonstrated that molecular concentration at the surface of a graphene FET can be continuously and reversibly manipulated via a back-gate voltage applied simultaneously with source-drain current. The equilibrium molecular concentration is precisely determined by the capacitance between the back-gate electrode and the graphene, in combination with the energy difference between the Dirac point and the molecular LUMO level. The driving force behind this dynamic mechanical reconfiguration of molecular concentration is the energetic favorability of molecular Fermi level pinning compared to filling the graphene Dirac bands. The energy alignment of the molecular LUMO level obtained from a concentration-based analysis using these concepts compares well with the value determined from STS.

■ ASSOCIATED CONTENT

Supporting Information

The Supporting Information is available free of charge at <https://pubs.acs.org/doi/10.1021/acs.nanolett.1c03039>.

Experimental methods, characteristics of the graphene devices, and spectra fitting methodology (PDF)

■ AUTHOR INFORMATION

Corresponding Author

Michael F. Crommie – Department of Physics, University of California, Berkeley, California 94720, United States; Materials Sciences Division, Lawrence Berkeley National Laboratory, Berkeley, California 94720, United States; Kavli Energy NanoSciences Institute at the University of California, Berkeley, California 94720, United States; orcid.org/0000-0001-8246-3444; Email: crommie@berkeley.edu

Authors

Franklin Liou – Department of Physics, University of California, Berkeley, California 94720, United States; Materials Sciences Division, Lawrence Berkeley National Laboratory, Berkeley, California 94720, United States; Kavli Energy NanoSciences Institute at the University of California, Berkeley, California 94720, United States

Hsin-Zon Tsai – Department of Physics, University of California, Berkeley, California 94720, United States; Materials Sciences Division, Lawrence Berkeley National Laboratory, Berkeley, California 94720, United States

Andrew S. Aikawa – Department of Physics, University of California, Berkeley, California 94720, United States; Materials Sciences Division, Lawrence Berkeley National Laboratory, Berkeley, California 94720, United States

Kyler C. Natividad – Department of Physics, University of California, Berkeley, California 94720, United States

Eric Tang – Department of Physics, University of California, Berkeley, California 94720, United States

Ethan Ha – Department of Physics, University of California, Berkeley, California 94720, United States

Alexander Riss – Physics Department E20, Technical University of Munich, D-85748 Garching, Germany

Kenji Watanabe – Research Center for Functional Materials, National Institute for Materials Science, Tsukuba 305-0044, Japan; orcid.org/0000-0003-3701-8119

Takashi Taniguchi – International Center for Materials Nanoarchitectonics, National Institute for Materials Science, Tsukuba 305-0044, Japan; orcid.org/0000-0002-1467-3105

Johannes Lischner – Department of Materials, Imperial College London, London SW7 2BB, United Kingdom; orcid.org/0000-0002-9601-7821

Alex Zettl – Department of Physics, University of California, Berkeley, California 94720, United States; Materials Sciences Division, Lawrence Berkeley National Laboratory, Berkeley, California 94720, United States; Kavli Energy NanoSciences Institute at the University of California, Berkeley, California 94720, United States

Complete contact information is available at:

<https://pubs.acs.org/10.1021/acs.nanolett.1c03039>

Author Contributions

◆F.L. and H.-Z. T. contributed equally to this paper

Notes

The authors declare no competing financial interest.

ACKNOWLEDGMENTS

This research was supported by the Director, Office of Science, Office of Basic Energy Sciences, Materials Sciences and Engineering Division, of the U.S. Department of Energy under contract no. DE-AC02-05CH11231 (Nanomachine program-KC1203) (STM imaging and spectroscopy), by the Molecular Foundry (graphene growth, growth characterization), by the National Science Foundation grant DMR-1807233 (device fabrication). K.W. and T.T. acknowledge support from the Elemental Strategy Initiative conducted by the MEXT, Japan, Grant Number JPMXP0112101001 (characterization of BN crystals) and JSPS KAKENHI Grant Number JP20H00354 (growth of BN crystals). A.R. acknowledges funding by the Deutsche Forschungsgemeinschaft (DFG, German Research Foundation) 453903355 (data analysis). F.L. acknowledges support from Kavli ENSI Philomathia Graduate Student Fellowship.

REFERENCES

- (1) Feenstra, R. M.; Mårtensson, P. Fermi-Level Pinning at the Sb/GaAs(110) Surface Studied by Scanning Tunneling Spectroscopy. *Phys. Rev. Lett.* **1988**, *61*, 447–450.
- (2) Spicer, W. E.; Newman, N.; Spindt, C. J.; Lilienthal-Weber, Z.; Weber, E. R. “Pinning” and Fermi level movement at GaAs surfaces and interfaces. *J. Vac. Sci. Technol., A* **1990**, *8*, 2084–2089.
- (3) Grassman, T. J.; Bishop, S. R.; Kummel, A. C. An atomic view of Fermi level pinning of Ge(100) by O₂. *Surf. Sci.* **2008**, *602*, 2373–2381.
- (4) Hurdax, P.; Hollerer, M.; Puschnig, P.; Lüftner, D.; Egger, L.; Ramsey, M. G.; Sterrer, M. Controlling the Charge Transfer across Thin Dielectric Interlayers. *Adv. Mater. Interfaces* **2020**, *7*, 2000592.
- (5) Sharbati, M. T.; Du, Y.; Torres, J.; Ardolino, N. D.; Yun, M.; Xiong, F. Low-Power, Electrochemically Tunable Graphene Synapses for Neuromorphic Computing. *Adv. Mater.* **2018**, *30*, 1870273.
- (6) Cui, K.; Ivasenko, O.; Mali, K. S.; Wu, D.; Feng, X.; Müllen, K.; De Feyter, S.; Mertens, S. F. L. Potential-driven molecular tiling of a charged polycyclic aromatic compound. *Chem. Commun.* **2014**, *50*, 10376–10378.
- (7) Cai, Z. F.; Yan, H. J.; Wang, D.; Wan, L. J. Potential- and concentration-dependent self-assembly structures at solid/liquid interfaces. *Nanoscale* **2018**, *10*, 3438–3443.
- (8) Wickenburg, S.; Lu, J.; Lischner, J.; Tsai, H.-Z.; Omrani, A. A.; Riss, A.; Karrasch, C.; Bradley, A.; Jung, H. S.; Khajeh, R.; et al.

Tuning charge and correlation effects for a single molecule on a graphene device. *Nat. Commun.* **2016**, *7*, 13553.

- (9) Pinto, H.; Jones, R.; Goss, J. P.; Briddon, P. R. p-type doping of graphene with F4-TCNQ. *J. Phys.: Condens. Matter* **2009**, *21*, 402001.
- (10) Barja, S.; Garnica, M.; Hinarejos, J. J.; Vázquez De Parga, A. L.; Martin, N.; Miranda, R. Self-organization of electron acceptor molecules on graphene. *Chem. Commun.* **2009**, *46*, 8198–8200.
- (11) Khomyakov, P. A.; Giovannetti, G.; Rusu, P. C.; Brocks, G.; Van Den Brink, J.; Kelly, P. J. First-principles study of the interaction and charge transfer between graphene and metals. *Phys. Rev. B: Condens. Matter Mater. Phys.* **2009**, *79*, 195425.
- (12) Kumar, A.; Banerjee, K.; Dvorak, M.; Schulz, F.; Harju, A.; Rinke, P.; Liljeroth, P. Charge-Transfer-Driven Nonplanar Adsorption of F4TCNQ Molecules on Epitaxial Graphene. *ACS Nano* **2017**, *11*, 4960–4968.
- (13) Coletti, C.; Riedl, C.; Lee, D. S.; Krauss, B.; Patthey, L.; Von Klitzing, K.; Smet, J. H.; Starke, U. Charge neutrality and band-gap tuning of epitaxial graphene on SiC by molecular doping. *Phys. Rev. B: Condens. Matter Mater. Phys.* **2010**, *81*, 235401.
- (14) Akiyoshi, H.; Goto, H.; Uesugi, E.; Eguchi, R.; Yoshida, Y.; Saito, G.; Kubozono, Y. Carrier Accumulation in Graphene with Electron Donor/Acceptor Molecules. *Advanced Electronic Materials* **2015**, *1*, 1500073.
- (15) Lu, J.; Tsai, H.-Z.; Tatan, A. N.; Wickenburg, S.; Omrani, A. A.; Wong, D.; Riss, A.; Piatti, E.; Watanabe, K.; Taniguchi, T.; et al. Frustrated supercritical collapse in tunable charge arrays on graphene. *Nat. Commun.* **2019**, *10*, 477.
- (16) Tsai, H.-Z.; Lischner, J.; Omrani, A. A.; Liou, F.; Aikawa, A. S.; Karrasch, C.; Wickenburg, S.; Riss, A.; Natividad, K. C.; Chen, J.; Choi, W.-W.; Watanabe, K.; Taniguchi, T.; Su, C.; Louie, S. G.; Zettl, A.; Lu, J.; Crommie, M. F. A molecular shift register made using tunable charge patterns in one-dimensional molecular arrays on graphene. *Nature Electronics* **2020**, *3*, 598–603.
- (17) Tsai, H. Z.; Omrani, A. A.; Coh, S.; Oh, H.; Wickenburg, S.; Son, Y. W.; Wong, D.; Riss, A.; Jung, H. S.; Nguyen, G. D.; Rodgers, G. F.; Aikawa, A. S.; Taniguchi, T.; Watanabe, K.; Zettl, A.; Louie, S. G.; Lu, J.; Cohen, M. L.; Crommie, M. F. Molecular Self-Assembly in a Poorly Screened Environment: F4TCNQ on Graphene/BN. *ACS Nano* **2015**, *9*, 12168–12173.
- (18) Pavliček, N.; Swart, I.; Niedenfür, J.; Meyer, G.; Repp, J. Symmetry dependence of vibration-assisted tunneling. *Phys. Rev. Lett.* **2013**, *110*, 136101.
- (19) Qiu, X. H.; Nazin, G. V.; Ho, W. Vibronic states in single molecule electron transport. *Phys. Rev. Lett.* **2004**, *92*, 206102.
- (20) Zhang, Y.; Brar, V. W.; Wang, F.; Girit, C.; Yayon, Y.; Panlasigui, M.; Zettl, A.; Crommie, M. F. Giant phonon-induced conductance in scanning tunnelling spectroscopy of gate-tunable graphene. *Nat. Phys.* **2008**, *4*, 627–630.
- (21) Decker, R.; Wang, Y.; Brar, V. W.; Regan, W.; Tsai, H.-Z.; Wu, Q.; Gannett, W.; Zettl, A.; Crommie, M. F. Local Electronic Properties of Graphene on a BN Substrate via Scanning Tunneling Microscopy. *Nano Lett.* **2011**, *11*, 2291–2295.
- (22) Castro Neto, A. H.; Guinea, F.; Peres, N. M. R.; Novoselov, K. S.; Geim, A. K. The electronic properties of graphene. *Rev. Mod. Phys.* **2009**, *81*, 109–162.
- (23) Järvinen, P.; Hämäläinen, S. K.; Banerjee, K.; Häkkinen, P.; Ijäs, M.; Harju, A.; Liljeroth, P. Molecular self-assembly on graphene on SiO₂ and h-BN substrates. *Nano Lett.* **2013**, *13*, 3199–3204.
- (24) Cochrane, K. A.; Schiffrin, A.; Roussy, T. S.; Capsoni, M.; Burke, S. A. Pronounced polarization-induced energy level shifts at boundaries of organic semiconductor nanostructures. *Nat. Commun.* **2015**, *6*, 8312.